**Astronomy
&
Astrophysics**

The HARPS search for southern extra-solar planets

V. A 14 Earth-masses planet orbiting HD 4308[⋆]

S. Udry[1], M. Mayor[1], W. Benz[2], J.-L. Bertaux[3], F. Bouchy[4], C. Lovis[1],
C. Mordasini[2], F. Pepe[1], D. Queloz[1], and J.-P. Sivan[4]

[1] Observatoire de Genève, 51 Ch. des Maillettes, 1290 Sauverny, Switzerland
 e-mail: stephane.udry@obs.unige.ch
[2] Physikalisches Institut Universität Bern, Sidlerstrasse 5, 3012 Bern, Switzerland
[3] Service d'Aéronomie du CNRS, BP 3, 91371 Verrières-le-Buisson, France
[4] Laboratoire d'Astrophysique de Marseille, Traverse du Siphon, 13013 Marseille, France

ABSTRACT

We present here the discovery and characterisation of a very light planet around HD 4308. The planet orbits its star in 15.56 days. The circular radial-velocity variation presents a tiny semi-amplitude of 4.1 m s^{-1} that corresponds to a planetary minimum mass $m_2 \sin i = 14.1$ $M_{\oplus}$ (Earth masses). The planet was unveiled by high-precision radial-velocity measurements obtained with the HARPS spectrograph on the ESO 3.6-m telescope. The radial-velocity residuals around the Keplerian solution are 1.3 m s^{-1}, demonstrating the very high quality of the HARPS measurements. Activity and bisector indicators exclude any significant perturbations of stellar intrinsic origin, which supports the planetary interpretation. Contrary to most planet-host stars, HD 4308 has a marked sub-solar metallicity ([Fe/H] = −0.31), raising the possibility that very light planet occurrence might show a different coupling with the parent star's metallicity than do giant gaseous extra-solar planets. Together with Neptune-mass planets close to their parent stars, the new planet occupies a position in the mass-separation parameter space that is constraining for planet-formation and evolution theories. The question of whether they can be considered as residuals of evaporated gaseous giant planets, ice giants, or super-earth planets is discussed in the context of the latest core-accretion models.

Key words. stars: individual: HD 4308 – methods: observational – techniques: radial velocities – techniques: spectroscopic – instrumentation: spectrographs

1. Introduction

After a decade of enthusiastic discoveries in the field of extra-solar gaseous giant planets, mainly coming from large high-precision radial-velocity surveys of solar-type stars, the *quest for other worlds* has now passed a new barrier with the recent detections of several planets in the Neptune-mass regime (McArthur et al. 2004; Santos et al. 2004b; Butler et al. 2004; Vogt et al. 2005; Rivera et al. 2005; Bonfils et al. 2005). They are supposedly mainly composed of icy/rocky material, being formed without or having lost the extended gaseous atmosphere expected to grow during the planet migration towards the centre of the system.

This new step forward has been made possible primarily thanks to the development of a new generation of instruments capable of radial-velocity measurements of unprecedented quality. The "fer de lance" among them is undoubtedly the

ESO high-resolution HARPS fiber-fed echelle spectrograph especially designed for planet-search programmes and asteroseismology. HARPS has already proved to be the most precise spectro-velocimeter to date, as it reaches an instrumental radial-velocity accuracy at the level of 1 m s^{-1} over months/years (Mayor et al. 2003; Lovis et al. 2005). The precision achieved is even better on a short-term basis (Bouchy et al. 2005). Another fundamental change that has allowed this progress in planet detection towards the very low masses is the application of a careful observing strategy to reduce as much as possible the perturbing effect of stellar oscillations hiding the tiny radial-velocity signal induced on solar-type stars by Neptune-mass planets. This is discussed further in detail in Sect. 3.

In about 1.5 years, the GTO HARPS planet-search programme has discovered (or co-discovered) 11 planets, amongst which there are: 5 hot Jupiters (Pepe et al. 2004; Moutou et al. 2005; Lo Curto et al. 2006); 3 planets with masses in the sub-Saturn mass regime and orbiting at moderate distances from their parent stars (Lovis et al. 2005); and 3 Neptune-mass

---

[⋆] Based on observations made with the HARPS instrument on the ESO 3.6 m telescope at La Silla Observatory under the GTO programme ID 072.C-0488.
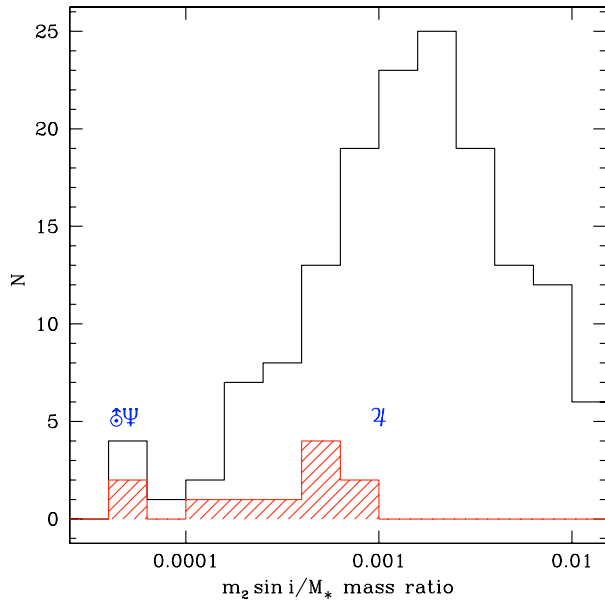
Fig. 1. Distribution of planet to primary-star mass ratios for the known exoplanets and low-mass brown dwarfs. The HARPS detections are represented by the hatched histogram. Planet symbols indicate the positions of Jupiter-, Neptune-, and Uranus-mass objects.

Table 1. Observed and inferred parameters of HD 4308. Photometric and astrometric parameters were taken from the Hipparcos catalogue (ESA 1997). The other stellar physical quantities were obtained from a high-resolution ETL spectral analysis or were interpolated in the grid of Geneva evolution models (Schaerer et al. 1993).

Parameter		HD 4308
Sp		G5V
V	[mag]	6.54
$B - V$	[mag]	0.65
π	[mas]	45.76
M_V	[mag]	4.85
T_{eff}	[K]	5685 ± 13
$\log g$	[cgs]	4.49 ± 0.07
[Fe/H]	[dex]	-0.31 ± 0.01
L	[$L_\odot$]	0.99
M_*	[$M_\odot$]	0.83 ± 0.01
$v \sin i$	[km s^{-1}]	1.2
$\log R'_{\mathrm{HK}}$		-4.93
P_{rot} ($\log R'_{\mathrm{HK}}$)	[days]	24
age (model/$\log R'_{\mathrm{HK}}$)	[Gyr]	$>10 / 4.3$

planets, namely a 14.4 $M_\oplus$ planet around μ Ara (Santos et al. 2004b), a 16.6 $M_\oplus$ planet around the M3 Gl 581 (Bonfils et al. 2005), and the planet described in this paper. As illustrated in Fig. 1, these planets lie mainly in the low-mass tail of the planetary-mass distribution. This distribution, which was known to be biased towards low masses, can now be explored in greater detail. The characterisation of the low-mass objects will strongly constrain planet-formation and evolution scenarios, as planets with masses between 10 and 100 $M_\oplus$ are not expected in large numbers according to some current formation models (see e.g. Ida & Lin 2004a).

The discovery of the extremely low-mass planets represents a new benchmark for planet surveys and provides information on the low end of the planetary-mass distribution. In this paper, we present the discovery of a new very low-mass companion to the star HD 4308. Interesting characteristics of this planet include its Uranus-like mass and the low metallicity of its parent star. The paper is structured as follows. Section 2 briefly describes the physical properties of the parent star. The radial-velocity measurements, observation strategy, and orbital solution are presented in Sects. 3 and 4. Finally, we discuss the characteristics of the new planet in Sect. 5 in the context of the latest core-accretion planet-formation models, whereas the last section is devoted to some concluding remarks.

2. Stellar characteristics of HD 4308

The basic photometric (G5V, $V = 6.54$, $B - V = 0.65$) and astrometric ($\pi = 45.76$ mas) properties of HD 4308 were taken from the Hipparcos catalogue (ESA 1997). They are recalled in Table 1, together with inferred quantities like the absolute magnitude ($M_V = 4.85$) and the stellar physical characteristics derived from the HARPS spectra following the method described

in Santos et al. (2001, 2004a, 2005). A standard local thermodynamical equilibrium (LTE) analysis was applied to a *resulting* spectrum built as the sum of the 205 individual spectra gathered for the star (see next section). On this resulting spectrum, we measured an equivalent S/N of ~1100 in the Li wavelength region (6700 Å). This study thus provides very precise values for the effective temperature ($T_{\mathrm{eff}} = 5686 \pm 13$), metallicity ([Fe/H] $= -0.31 \pm 0.01$), and surface gravity ($\log g = 4.49 \pm 0.07$) of the star. The quoted uncertainties do not include systematic errors, such as the use of different temperature scales. However, these systematic errors should be small, in particular the ones concerning stellar metallicity (see discussion in Santos et al. 2004a, 2005).

Very interestingly, HD 4308 has a sub-solar metallicity contrary to most planet-host stars. The high values of the spatial velocities of the star ($U = -52$ km s^{-1}; $V = -110$ km s^{-1}; $W = -29$ km s^{-1}) further points towards the star probably belonging to the thick disk.

From the colour index, the derived effective temperature, and the corresponding bolometric correction, we estimated the star luminosity as 0.99 $L_\odot$. Except for its metallicity, the star is thus very similar to the Sun. Because of the low metallicity, however, we interpolated a sub-solar mass ($M_\star = 0.83\ M_\odot$) in the grid of Geneva stellar evolutionary models with appropriate metal abundance (Schaerer et al. 1993). The age derived from the model also points towards an old star (age > 10 Gyr). The projected rotational velocity $v \sin i = 1.2$ km s^{-1} was estimated using the calibration of the CORALIE cross-correlation function given in Santos et al. (2002). Table 1 gathers those values as well.

We also computed the $\log R'_{\mathrm{HK}}$ activity indicator from the spectra, measuring the re-emission flux in the Ca II H and K lines corrected for the photospheric flux contribution. This index represents a useful tool for estimating the stellar
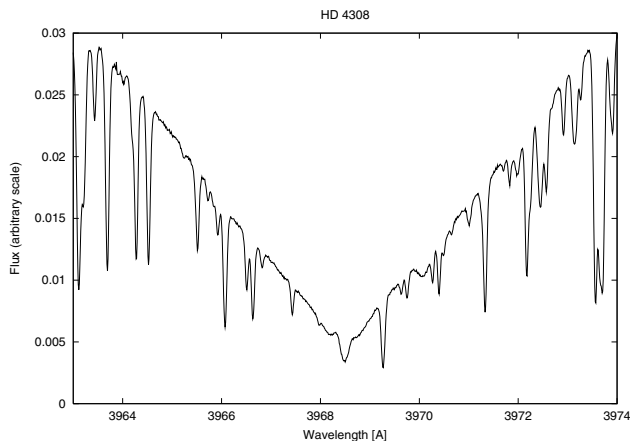
Fig. 2. Ca II H (λ = 3968.47 Å) absorption line region of the summed HARPS spectra for HD 4308. Re-emission in the core of the line is absent, showing the low chromospheric activity of the star.
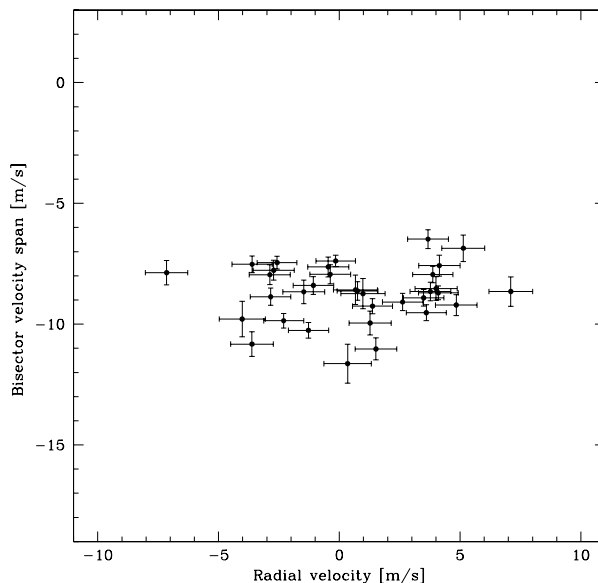

Fig. 3. Bisector velocity span as a function of the measured radial velocity. No correlation is found supporting a non-intrinsic origin for the radial-velocity variation.

radial-velocity jitter expected for the star due to rotational modulation of star spots or other active regions on the stellar surface (Saar & Donahue 1997; Santos et al. 2000). From this indicator we derived a stellar rotation period P_{rot} = 24 days (following Noyes et al. 1984), as well as an activity-based age estimate of ~4.3 Gyr (from the calibration by Donahue 1993; Henry et al. 1996)[1]. HD 4308 was found to be non-active as shown by the low value of $\log R'_{HK}$ = −4.93[2] and the absence of re-emission observed in the core of the CaII H line displayed in Fig. 2. Together with the measured small $v \sin i$, these features indicate very low activity-induced radial-velocity jitter for this star. Moreover, analysis of the bisector shape of the cross-correlation function (see details on the method in Queloz et al. 2001) shows no variations in the CCF profile down to the photon noise level (Fig. 3), giving strong support to a planetary origin of the radial-velocity variations.

3. Very high precision radial-velocity measurements and observing strategy

HD 4308 is part of the HARPS "high-precision" GTO subsample that aims at detecting very low-mass extra-solar planets by pushing the radial velocity measurement accuracy below the 1 m s^{-1} mark. However, asterosismology observations carried out by HARPS have made clear that the precision the instrument is capable of achieving is no longer set by instrumental characteristics but rather by the stars themselves (Mayor et al. 2003; Bouchy et al. 2005). Indeed, stellar p-mode oscillations on short time-scales and stellar jitter on longer time-scales can and do induce significant radial-velocity changes at the level of accuracy of HARPS measurements. For instance, even a very "quiet" G or K dwarf shows oscillation modes of several tens of cm s^{-1} each, which might add up to radial-velocity

amplitudes as large as several m s^{-1} (Bouchy et al. 2005). As a consequence, any exposure with a shorter integration time than the oscillation period of the star, or even than mode-interference variation time-scales, might fall arbitrarily on a peak or on a valley of these mode interferences and thus introduce additional radial-velocity "noise". This phenomenon could, therefore, seriously compromise the ability to detect very low-mass planets around solar-type stars by means of the radial-velocity technique.

To minimize these effects as much as possible, the stars of the HARPS GTO "high-precision" sample have been selected from the CORALIE planet-search sample (Udry et al. 2000) as slowly rotating, non-evolved, and low-activity stars with no obvious radial-velocity variations at the CORALIE precision level (typically 10 m s^{-1} for HD 4308). Moreover, in order to average out stellar oscillations, the observations are designed to last at least 15 min on the target, splitting them in several exposures, when required, to avoid CCD saturation. The radial velocities of individual exposures are obtained with the standard HARPS reduction pipeline, based on the cross-correlation with an appropriate stellar template, the precise nightly wavelength calibration with ThAr spectra and the tracking of instrumental drifts with the simultaneous ThAr technique (Baranne et al. 1996). The final radial velocity is then obtained by averaging the multiple consecutive exposures.

This strategy is now applied to all stars in the "high-precision" programme. The results are best summarised by the histogram of the radial-velocity dispersion of the HARPS measurements for this programme (Fig. 4). The distribution mode is just below 2 m s^{-1}, and the peak decreases rapidly towards higher values. More than 80% of the stars show smaller dispersion than 5 m s^{-1}, and more than 35% have dispersions below 2 m s^{-1}. It must be noted that the computed dispersion includes photon-noise error, wavelength-calibration error, stellar oscillations and jitter, and, in particular, it is "polluted" by
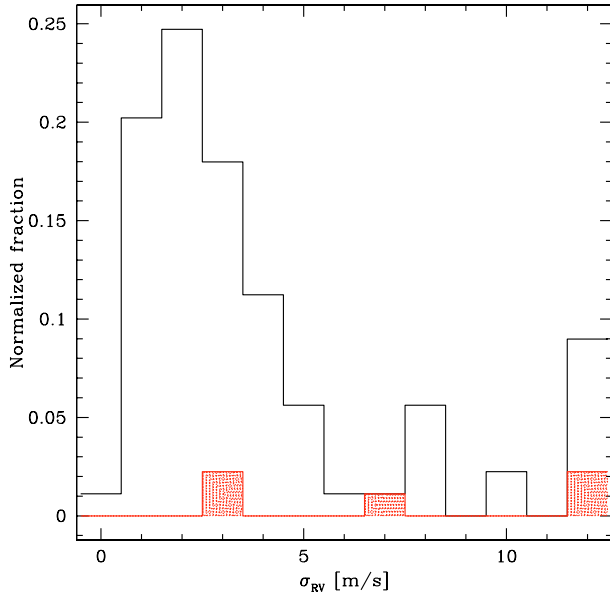
---

[1] Although the relation has been shown not to be reliable for ages greater than ~2 Gyr (Pace & Pasquini 2004), it is still helpful to distinguish between active, young stars and chromospherically quiet, old stars.

[2] A value $\log R'_{HK}$ = −5.05 is given in Henry et al. (1996) leading to an age estimate of 6.3 Gyr.

Fig. 4. Histogram of the observed radial-velocity dispersion (σ_{RV}) of the stars in the HARPS "high-precision" sub-programme. It has been produced using the data obtained with the new observing strategy and includes only stars with more than 3 measurements. The position of the planets detected with HARPS is indicated by the hatched area.

known extrasolar planets (hatched part in Fig. 4) and still undetected planetary companions.

4. Orbital Keplerian solution for HD 4308 b

A set of 205 individual high S/N spectra covering 680 days were gathered for HD 4308, as described in Sect. 3. They finally corresponded to 41 radial-velocity measurements after the multiple-exposure averages. Typical exposure times of 5 min yielded S/N ratios of ~150 per pixel at 550 nm for individual spectra, corresponding to individual photon-noise errors of ~0.5 m s^{-1}. After combining the spectra, we quadratically added the night wavelength calibration error[3]. The list of the averaged radial-velocity measurements obtained for HD 4308 is given in Table 2.

The intermediate-season velocities are displayed in Fig. 5 with the best Keplerian solution fitted to the data. The derived period is 15.56 days, and the radial-velocity semi-amplitude K is 4.1 m s^{-1}. Despite the small amplitude of the radial-velocity variation, we estimated a small false-alarm probability for the period derived of 10^{-3} from Monte-Carlo simulations. The best Keplerian planetary solution is circular. Considering a primary mass of 0.83 $M_\odot$, these parameters lead to a minimum mass $m_2 \sin i = 0.0442 \, M_{Jup} = 14.1 \, M_\oplus$ and a separation $a = 0.115$ AU for the planet. Figure 6 shows the radial velocities folded to the orbital period, including 3 older "single-shot" measurements obtained before the change in our observational

[3] Presently on the order of 80 cm s^{-1}, this error represents the main limitation on the measurement precision, but it will improve soon thanks to an ongoing redefinition of the thorium lines used for the wavelength calibration. See also Lovis et al. (2005) for further details on the different error sources of the radial-velocity estimate.

Table 2. Multiple-exposure averaged radial-velocities and uncertainties (including calibration errors) for HD 4308. All data are relative to the solar system barycentre.

JD-2 400 000	RV	Uncertainty
[days]	[km s^{-1}]	[km s^{-1}]
52 899.77052	95.24540	0.00136
52 939.67749	95.25140	0.00144
52 946.72659	95.24100	0.00157
53 266.77155	95.24955	0.00102
53 268.72143	95.24940	0.00100
53 273.74140	95.24154	0.00100
53 274.74846	95.24200	0.00095
53 287.69258	95.24542	0.00101
53 288.69001	95.24426	0.00088
53 289.70387	95.24530	0.00089
53 291.68596	95.23983	0.00109
53 292.67405	95.24129	0.00092
53 294.64135	95.24244	0.00115
53 295.76250	95.24850	0.00129
53 298.72754	95.24822	0.00090
53 308.68463	95.24248	0.00088
53 309.54646	95.24317	0.00095
53 310.65747	95.24471	0.00088
53 312.54143	95.24896	0.00094
53 314.70856	95.24910	0.00094
53 315.62201	95.24953	0.00094
53 321.64168	95.23840	0.00116
53 366.54310	95.24383	0.00087
53 367.58691	95.24281	0.00088
53 371.56598	95.24321	0.00088
53 372.55973	95.24643	0.00088
53 373.55895	95.24720	0.00094
53 374.55931	95.24707	0.00090
53 376.54410	95.24964	0.00088
53 377.53686	95.24710	0.00089
53 401.53108	95.24470	0.00126
53 403.54910	95.24422	0.00100
53 404.52408	95.24675	0.00099
53 406.52597	95.24824	0.00100
53 408.52500	95.25076	0.00105
53 409.52594	95.24960	0.00101
53 410.52003	95.24961	0.00100
53 412.50936	95.24525	0.00101
53 573.91705	95.24330	0.00112
53 576.87555	95.24970	0.00111
53 579.83685	95.24990	0.00115

strategy. Orbital and inferred parameters for the non-circular solution are given in Table 3.

The weighted rms of the residuals around the solution is 1.3 m s^{-1}, which is larger than the internal errors; but, as in the case of μ Ara (Santos et al. 2004b), they are most probably due to residuals of unaveraged stellar oscillation modes (Bouchy et al. 2005). No additional trend of the radial velocities is expected, as CORALIE measurements show that the star is constant at a 10 m s^{-1} level over close to 5 years.
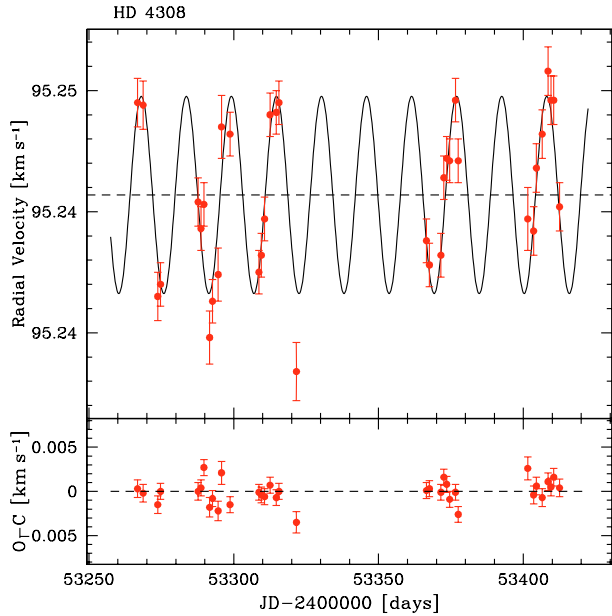
Fig. 5. Intermediate season of HARPS radial velocities for HD 4308. The best Keplerian fit to the data (solid curve) gives a minimum mass of 14.1 $M_\oplus$ and an orbital period of 15.56 days for the planet.
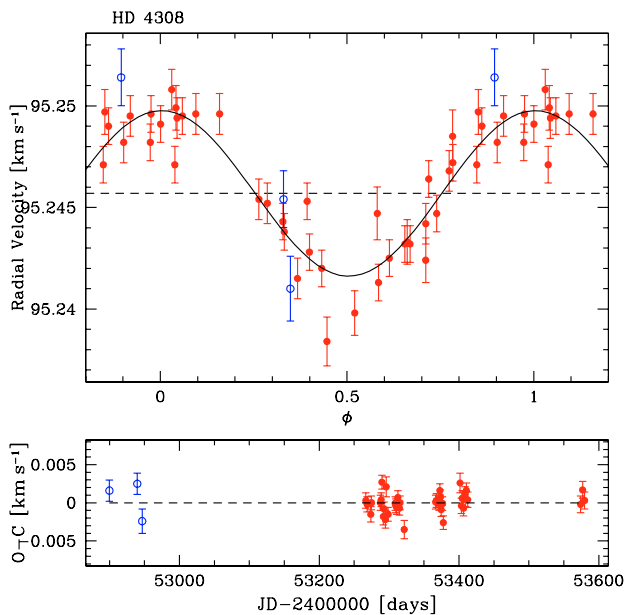

Fig. 6. Phase-folded radial velocities of HD 4308 superimposed on the best Keplerian orbital solution (solid curve). The 3 older points obtained before introducing the new observing strategy (see text) are indicated by open symbols.

5. Discussion

5.1. Constraining formation and evolution scenarios

Low-mass giant planets, i.e. planets with masses in the range 10–100 $M_\oplus$, are particularly interesting as they provide potentially strong constraints on current models of giant planet formation and evolution. Indeed, and perhaps contrary to intuition, the formation of these objects within the current theoretical models appears more difficult than the formation of

Table 3. Orbital and physical parameters for HD 4308 b.

Parameter		HD 4308 b
P	[days]	15.56 ± 0.02
T	[JD-2 400 000]	53314.70 ± 2.0
e		$0.00 + 0.01$
V	[km s^{-1}]	95.2457 ± 0.0002
ω	[deg]	359 ± 47
K	[m s^{-1}]	4.07 ± 0.2
$a_1 \sin i$	[10^{-6} AU]	5.826
$f(m)$	[$10^{-13}\ M_\odot$]	1.09
$m_2 \sin i$	[$M_{\rm Jup}$]	0.0442
a	[AU]	0.115
$N_{\rm meas}$		41
Span	[days]	680
σ (O–C)	[m s^{-1}]	1.3
$\chi^2_{\rm red}$		1.92

their more massive counterparts. For this reason, objects with masses within or at the edge of this range, like μ Ara c and HD 4308 b, are especially interesting.

In the direct collapse scenario, planets form through gravitational collapse of patches of the proto-planetary disk (Boss 2002) on very short timescales. High-resolution simulations (Mayer et al. 2002, 2005) of this process show that planets tend to form on elliptical orbits with a semi-major axis of several astronomical units and masses between 1 and 7 $M_{\rm Jup}$. In this scenario, μ Ara-type planets would have to result from the subsequent evolution involving migration and from a very significant amount of mass loss.

In the framework of the core accretion model (e.g. Pollack et al. 1996), the final mass of a planet is actually determined by the amount of gas the core accretes after it has reached a critical mass, which is about 10–15 $M_\oplus$. In Ida & Lin (2004a), this amount is determined by the rate at which gas can be accreted (essentially the Kelvin-Helmholtz timescale) and by the total amount of gas available within the planet's gravitational reach. Since for super-critical cores the Kelvin-Helmholtz timescale is short and the amount of gas available large (compared to an Earth's mass) even in low mass disks, planets tend to form either less or significantly more massive than the critical mass. From a large number of formation model calculations, Ida & Lin (2004a) have found that only very few planets form in the mass range 10–100 $M_\oplus$, a range they actually call *a planetary desert*.

In the extended core accretion models by Alibert et al. (2005), the planet should be able to accrete gas over the entire lifetime of the disk, due to its migration. However, since the latter thins out with time and the planet eventually opens a gap as it grows more massive, the gas supply decreases with time. The growth rate of the planet is actually set by the rate at which the disk can supply the gas rather than by the rate at which the planet can accrete it. Monte Carlo simulations are ongoing to

check whether these models lead to a different planetary initial mass function than in Ida & Lin (2004a).

At first glance, the relatively numerous small-mass objects discovered so far seem to pose a problem for current planet formation theories (Lovis et al. 2005); however, the situation is actually more complex. For example, examining a potential metallicity-mass relation for exoplanets, Rice & Armitage (2005) raise the possibility that the planet desert might be populated by late-forming planets for which the evolution/migration is stopped at intermediate masses and distances by the dissolution of the disk. Also, since all the very low-mass planets that are currently known are located close to their star, one cannot exclude the possibility that these objects were initially much more massive and then have lost a significant amount of their mass through evaporation during their lifetime (see Baraffe et al. 2004, 2005, for a more detailed discussion).

While mass loss from initially more massive objects could possibly account for the light planets very close to their star, it is not clear whether μ Ara c located at a distance of 0.09 AU could actually result from the evaporation of a more massive object. The situation is even more critical for HD 4308 b that is located farther away (0.115 AU) from its parent star, which is, in addition, less luminous than μ Ara by a factor of ~1.8. The effects could possibly be compensated for, at least partially, by the estimated very old age of the star. However, as more μ Ara-like objects are being discovered, and if they are all the results of the evaporation of larger mass planets, the question of the probability of detecting these systems shortly before complete evaporation will become a central one. As already stated by Baraffe et al. (2005), the current evaporation models are still affected by large uncertainties – lack of detailed chemistry, non-standard chemical composition in the envelope, effect or rocky/icy cores, etc. – that will need to be clarified in order to solve the question of the possible formation of μ Ara-type planets through evaporation.

Finally, given their close location to their star, the detected small mass planets are likely to have migrated to their current position from further out in the nebula. The chemical composition of these planets will depend upon the extent of their migration and the thermal history of the nebula and, hence, on the composition of the planetesimals along the accretion path of the planet. The situation is complicated by the fact that the iceline itself is moving as the nebula evolves (see e.g. Sasselov & Lecar 2000). Detailed models of planetary formation that include these effects have yet to be developed.

5.2. Influence of parent star metallicity

It is well-established that the detected giant planets preferentially orbit metal-rich stars (Gonzalez 1998; Gonzalez & Vanture 1998; Gonzalez et al. 2001; Santos et al. 2001, 2003, 2005; Fischer & Valenti 2005). The frequency of planets is even found to be a steeply rising function of the parent star's metallicity, as soon as the latter is over solar (Santos et al. 2001; Fischer & Valenti 2005). In the scenario where gas giants acquire their mass through planetesimal coagulation followed by rapid gas accretion onto the core, the high probability of a
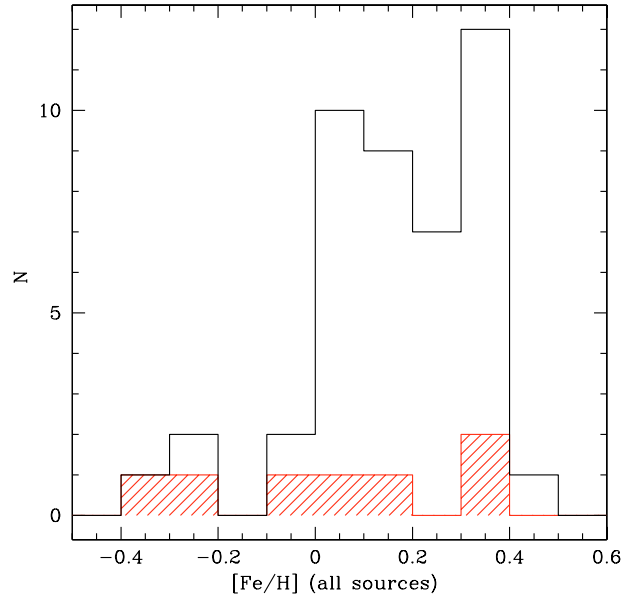

Fig. 7. Metallicity distribution of the sample of extrasolar planet hosts for planets with shorter periods than 20 days. Stars with Neptune-mass planets are indicated by the shaded histogram.

planet to be present around metal-rich stars arises naturally[4] if protostellar disks attain the same fraction of heavy material as the forming central star (Ida & Lin 2004b).

If the new *hot Neptune* planets are the remains of evaporated ancient giant planets, they should also follow the metallicity trend of their giant progenitors. This does not seem to be the case, considering that the 7 known planets with $m_2 \sin i \leq 21\,M_\oplus - \mu$ Ara c (Santos et al. 2004b), 55 Cnc (McArthur et al. 2004), Gl 436 (Butler et al. 2004), Gl 777A c (Vogt et al. 2005), Gl 876 d (Rivera et al. 2005), Gl 581 (Bonfils et al. 2005), and HD 4308 b – have metallicities of 0.33, 0.35, 0.02, 0.14, −0.03, −0.25, and −0.31, respectively. Although the statistics are still poor, the spread of these values over the nearly full range of planet-host metallicities (Fig. 7) suggests a different relation between metal content and planet frequency for the icy/rocky planets in regard to the giant ones.

However, we have to note here that 3 of the candidates orbit M-dwarf primaries. Recent Monte-Carlo simulations by Ida & Lin (2005) show that planet formation around small-mass primaries tends to form planets with lower masses in the Uranus/Neptune domain. A similar result that favours lower-mass planets is also observed for solar-type stars in the case of the low metallicity of the protostellar nebula (Ida & Lin 2004b; Mordasini et al. in prep.). Future improvements in the planet-formation models and new detections of very-low mass planets will help to better understand these 2 converging effects.

6. Summary and concluding remarks

In this paper we have reported the detection of a new very light planet in the Uranus/Neptune mass range that orbits the

---

[4] On the contrary, such a correlation is not expected with the gravitational-instability scenario. Recent simulations even lead to the opposite result (Cai et al. 2005).

deficient star HD 4308. With a period of 15.56 days (a = 0.115 AU), the planet is very similar to μ Ara c (Santos et al. 2004b). This new discovery was made possible by the high radial-velocity precision reached with the HARPS spectrograph and the applied observing strategy of averaging down the intrinsic radial-velocity "noise" induced by stellar oscillation modes. The HARPS precision is demonstrated by the very low residuals around the orbital fit, allowing for accurate determination of the orbital parameters.

The existence of small planets (10–100 $M_\oplus$) at short and intermediate distances from their stars strongly constrains the standard planet formation and evolution theories. The difficulty arises from the fast runaway accretion and the potentially large amount of gas available for accretion, both leading towards larger mass planets whose inward migration should turn them into hot Jupiters (or hot Saturns). However, other effects, such as metallicity (and HD 4308 is metal deficient), have not yet been studied in detail.

Evaporation could possibly be invoked to account for the planets that are very close to their star (Baraffe et al. 2004, 2005). However, it is not clear whether μ Ara b, and especially HD 4308b, could actually result from the evaporation of a more massive object. In the case of negligible evaporation or if other small mass planets should be discovered for which evaporation can safely be ruled out, the existence of the "planetary desert", or at least its depth, must be questioned. Therefore, from an observational point of view, a larger sample of small objects far enough away from the star, would be of paramount importance for further constraining our understanding of the formation of giant planets.

Recent HARPS discoveries indicate that a population of Neptune- and Saturn-mass planets remains to be discovered below 1 AU. The increasing precision of the radial-velocity surveys will help answer this question in the near future, thereby providing us with useful new constraints on planet formation theories. With the precision level achieved by HARPS, a new field in the search for extrasolar planets is now open, allowing the detection of companions of a few Earth masses around solar-type stars. Very low-mass planets ($<$10 $M_\oplus$) might be more frequent than the previously found giant worlds. Such planets will furthermore be preferential targets for space missions like the photometric satellites COROT and Kepler.

References

Alibert, Y., Mordasini, C., Benz, W., & Winisdoerffer, C. 2005, A&A, 434, 343

Baraffe, I., Selsis, F., Chabrier, G., et al. 2004, A&A, 419, L13

Baraffe, I., Chabrier, G., Barman, T., et al. 2005, A&A, 436, L47

Baranne, A., Queloz, D., Mayor, M., et al. 1996, A&AS, 119, 373

Bonfils, X., Forveille, T., Delfosse, X., et al. 2005, A&A, 443, L15

Boss, A. 2002, ApJ, 576, 462

Bouchy, F., Bazot, M., Santos, N., Vauclair, S., & Sosnowska, D. 2005, A&A, 440, 609

Butler, R., Vogt, S., Marcy, G., et al. 2004, ApJ, 617, 580

Cai, K., Durisen, R. H., Michael, S., et al. 2005, ApJ, 636, L149

Donahue, R. 1993, Ph.D. Thesis, New Mexico State University

ESA. 1997, The HIPPARCOS and TYCHO catalogue, ESA-SP, 1200

Fischer, D. A., & Valenti, J. 2005, ApJ, 622, 1102

Gonzalez, G. 1998, A&A, 334, 221

Gonzalez, G., & Vanture, A. 1998, A&A, 339, L29

Gonzalez, G., Laws, C., Tyagi, S., & Reddy, B. 2001, AJ, 121, 432

Henry, T., Soderblom, D., Donahue, R., & Baliunas, S. 1996, AJ, 111, 439

Ida, S., & Lin, D. 2004a, ApJ, 604, 388

Ida, S., & Lin, D. 2004b, ApJ, 616, 567

Ida, S., & Lin, D. 2005, ApJ, 626, 1045

Lo Curto, G., Mayor, M., Bouchy, F., et al. 2006, A&A, in press

Lovis, C., Mayor, M., Bouchy, F., et al. 2005, A&A, 437, 1121

Mayer, L., Quinn, T., Wadsley, J., & Stadel, J. 2002, Science, 298, 1756

Mayer, L., Wadsley, J., Quinn, T., & Stadel, J. 2005, MNRAS, 363, 361

Mayor, M., Pepe, F., Queloz, D., et al. 2003, The Messenger, 114, 20

McArthur, B., Endl, M., Cochran, W., et al. 2004, ApJ, 614, L81

Moutou, C., Mayor, M., Bouchy, F., et al. 2005, A&A, 439, 367

Noyes, R., Hartmann, L., Baliunas, S., Duncan, D., & Vaughan, A. 1984, ApJ, 279, 763

Pace, G., & Pasquini, L. 2004, A&A, 426, 1021

Pepe, F., Mayor, M., Queloz, D., et al. 2004, A&A, 423, 385

Pollack, J., Hubickyj, O., Bodenheimer, P., et al. 1996, Icarus, 124, 62

Queloz, D., Henry, G., Sivan, J., et al. 2001, A&A, 379, 279

Rice, W., & Armitage, P. 2005, ApJ, 630, 1107

Rivera, E., Lissauer, J., et al. 2005, ApJ, 634, 625

Saar, S., & Donahue, R. 1997, ApJ, 485, 319

Santos, N., Mayor, M., Naef, D., et al. 2000, A&A, 361, 265

Santos, N., Israelian, G., & Mayor, M. 2001, A&A, 373, 1019

Santos, N., Mayor, M., Naef, D., et al. 2002, A&A, 392, 215

Santos, N., Israelian, G., Mayor, M., Rebolo, R., & Udry, S. 2003, A&A, 398, 363

Santos, N., Israelian, G., & Mayor, M. 2004a, A&A, 415, 1153

Santos, N. C., Bouchy, F., Mayor, M., et al. 2004b, A&A, 426, L19

Santos, N., Israelian, G., Mayor, M., et al. 2005, A&A, 437, 1127

Sasselov, D., & Lecar, M. 2000, ApJ, 528, 995

Schaerer, D., Meynet, G., Maeder, A., & Schaller, G. 1993, A&AS, 98, 523

Udry, S., Mayor, M., Naef, D., et al. 2000, A&A, 356, 590

Vogt, S., Butler, P., Marcy, G., et al. 2005, ApJ, 632, 638